

---

## Supporting Information

# Post-Synthesis Modification of a Metal-Organic Framework to Construct a Bifunctional Photocatalyst for Hydrogen Production

Tianhua Zhou, Yonghua Du, Armando Borgna, Jindui Hong, Yabo Wang, Jianyu Han, Wei Zhang, and Rong Xu\*

### Materials and Methods.

Both 2,2'-bipyridine-5,5'-dicarboxylic acid and aluminum chloride hexahydrate ( $\text{AlCl}_3 \cdot 6\text{H}_2\text{O}$ ) were obtained from Sigma-Adrich and used as received. Potassium tetrachloroplatinate ( $\text{K}_2\text{PtCl}_4$ ), tetra(n-butyl) ammonium hexafluorophosphate ( $\text{n-Bu}_4\text{NPF}_6$ ) and triethanolamine (TEOA) were obtained from Alfa Aesar.  $\text{CH}_3\text{CN}$  was purchased from Kanto Chem. Co., Inc. All other solvents were obtained from Merck and used without further purification. *Cis*- $\text{Pt}(\text{DMSO})_2\text{Cl}_2$  was synthesized according to the procedure described in the literature.<sup>1</sup>  $\text{Pt}(\text{bpydc})\text{Cl}_2$  complex (bpydc = 2,2'-bipyridine-5,5'-dicarboxylic acid) was synthesized as previously described.<sup>2</sup>

Pt nanoparticles were synthesized by following the literature method.<sup>3</sup> Elemental analysis (C, H, N) was performed on an Elementary Vario El III instrument. FTIR spectra were obtained with a Perkin Elmer FT-IR Spectrum GX using KBr technique in the range of 4000–400  $\text{cm}^{-1}$ . Thermogravimetric analyses (TGA) were carried out with a TA Instruments TGA 5000 instrument at a heating rate of 15  $^\circ\text{C}/\text{min}$  under air atmosphere. Powder X-ray diffraction (XRD) patterns were obtained on a Bruker AXS D2 Advanced X-ray diffractometer with monochromatized Cu K $\alpha$  radiation ( $\lambda = 1.54056 \text{ \AA}$ , 40 kV and 20 mA). The data were collected with  $2\theta$  in a range of 5 $^\circ$ –65 $^\circ$  and a step size of 0.02 $^\circ/2\text{s}$ . All measurements were performed at room temperature and atmospheric pressure. An Agilent 7700x-MS Inductively Coupled Plasma-Mass Spectrometer (ICP-MS) was used to determine the Al and Pt contents. UV-Vis diffuse reflectance spectra were obtained by UV-visible absorption spectroscopy (UV-2450, Shimadzu). BET surface area was measured by  $\text{N}_2$  adsorption and desorption at 77 K using a Micromeritics ASAP 2020 apparatus and a Quantachrome Autosorb-6 sorption system. Samples of MOF-253 and MOF-253-Pt were degassed at offline at 250  $^\circ\text{C}$  and 120  $^\circ\text{C}$  for 16 h under vacuum before analysis.

### Fluorescence spectra

Fluorescence spectra of MOFs dispersed in 2 mL of degassed CH<sub>3</sub>CN/TEOA by ultrasonication were collected on a Fluoromax-3 spectrometer (Horiba Scientific). The concentration of TEOA was controlled at 0, 0.56, 1.13, 1.50 and 1.88 M, respectively.

### **Electrochemistry**

The electrochemical measurements were carried out on a CHI660C electrochemical workstation (CH Instruments, Shanghai Chenghua Co.) with a conventional three-electrode cell consisting of a Pt wire as a counter electrode. The saturated calomel electrode (SCE) was used as a reference electrode. Bu<sub>4</sub>NPF<sub>6</sub> (0.1 M) was selected as a supporting electrolyte. The working electrode was prepared as following: a glassy carbon electrode was polished with 0.05 μm Al<sub>2</sub>O<sub>3</sub>. Then, the electrode was ultrasonicated in ethanol and deionized water for 10 min, followed by drying at room temperature. MOF-253 or MOF-253-Pt (2 mg) was dispersed in 1 mL of ethanol and 0.5 mL of 0.05 wt% Naphthol and the resultant mixture was ultrasonicated for 5 min. Then, 0.06 mL of the mixture was casted onto the surface of the glassy carbon electrode and dried at room temperature. The apparent surface area of the electrode was 0.07 cm<sup>2</sup>. Prior to electrochemical experiments, the electrolyte was purged with high-purity nitrogen for at least 30 min to remove the dissolved oxygen. All experiments were performed in CH<sub>3</sub>CN solution at room temperature. The ferrocenium/ferrocene couple was measured to be 0.42 V. The photoelectrochemical measurement was carried out on a CHI660C electrochemical workstation with three-electrode cell with Pt plate as the counter electrode, SCE as the reference electrode, and MOF as the working electrode. The light source was a 300 W Xenon lamp with an appropriate cut-off filter. For the preparation of the MOF-253 or MOF-253-Pt electrode, MOF-253 or MOF-253-Pt (1 mg) was dispersed in 1 mL of ethanol and 0.5 mL of 0.05 wt% Naphthol and the resultant mixture was ultrasonicated. The suspension of MOF was deposited onto an indium-tin-oxide, dried at room temperature, and then dried at 333 K for 1 h. The photocurrents were recorded in 0.25 M Na<sub>2</sub>SO<sub>4</sub> aqueous solution containing 0.01 M TEOA under visible-light irradiation with a constant potential of 0.35 V versus SCE. The area irradiated was set at 0.19 cm<sup>2</sup>. The wavelength region of the irradiated light was controlled by using six different cut-off filters ( $\lambda > 400, 420, 455, 475, 500, \text{ and } 520$  nm).

### **Pt L<sub>III</sub>-edge X-ray absorption fine structure measurement**

Pt L<sub>III</sub>-edge XAFS spectra were recorded at room temperature in a fluorescence mode at XAFCA facility of ICES which is built in Singapore synchrotron light source (SSLS). A Si (III) double crystal was used to monochromatize the X-rays from the 2.5 GeV electron storage ring. In a typical experiment, the sample was prepared as a compressed pellet and

loaded into a cell. EXAFS data were examined by using the EXAFS analysis program, Rigaku EXAFS. The pre-edge peaks in the XANES regions were normalized for atomic absorption, based on the average absorption coefficient of the spectroscopic region. Fourier transformation of  $K_3$ -weighted normalized EXAFS data were performed over the range  $K = 3.5\text{--}12 \text{ \AA}$  to obtain the radial structure function. The CN (coordination number of scatters),  $R$  (distance between the absorbing atom and the scatterer), and Debye-Waller factor were estimated by curve-fitting analysis with inverse FT in the range  $R = 0.8\text{--}2.8 \text{ \AA}$  assuming single scattering.

### Synthesis of Al(OH)(bpydc) (MOF-253)

A mixture of  $\text{AlCl}_3 \cdot 6\text{H}_2\text{O}$  (151 mg, 0.625 mmol), glacial acetic acid (859  $\mu\text{L}$ , 15.0 mmol) and bpydc (153 mg, 0.625 mmol) (bpydc = 2,2'-bipyridine-5,5'-dicarboxylic acid) in 10 mL of  $N,N'$ -dimethylformamide (DMF) was placed in 20 mL of a Teflon-capped scintillation vial, stirred for 30 min, then heated at 120 °C for 24 h in an oil bath on a hotplate, and cooled to room temperature. After filtering, the resulting white powder was stirred in DMF at 80 °C for 3 h, followed by extracting with a Soxhlet extractor using methanol for 24 h and dried at 200 °C overnight in vacuum to give rise to  $\text{Al(OH)(bpydc)} \cdot 0.5\text{H}_2\text{O}$ . Yield: 145 mg (81%). Anal. Calcd for  $\text{C}_{12}\text{H}_7\text{AlN}_2\text{O}_5 \cdot 0.5\text{H}_2\text{O}$ : C, 48.82; H, 2.74; N, 9.49. Found: C, 48.58; H, 2.95; N, 9.22. IR (KBr,  $\text{cm}^{-1}$ ): 3426 (br), 1694 (w), 1593 (s), 1534 (w), 1480 (m), 1426 (s), 1289 (w), 1237 (w), 1170 (w), 1122 (w), 1050 (w), 1035(w), 997 (m), 854(w), 790 (s), 704 (m), 563(br).

### Synthesis of MOF-253-Pt (referring to MOF-253-0.5Pt unless otherwise stated)

The compounds  $\text{Al(OH)(bpydc)} \cdot 0.5\text{H}_2\text{O}$  (0.500g, 1.75 mmol) and *cis*-Pt(DMSO) $_2\text{Cl}_2$  (0.298 g, 0.71 mmol) were refluxed in acetonitrile (50 mL) under stirring for 15 h. After the mixture was cooled to room temperature, the yellow solid was obtained by filtration and stirred in 15 mL of acetonitrile at room temperature. After 24 h, the supernatant was decanted and repeated with the fresh acetonitrile. The solvent was exchanged twice for three days, followed by filtration and dried in vacuum at 60 °C to give rise to the yellow solid. Yield: 500 mg (62%). IR (solid-ATR): 3426 (br w), 1689 (w), 1599 (s), 1481 (m), 1427 (s), 1296 (w), 1242 (w), 1169 (w), 1125 (w), 1057 (w), 998 (w), 944 (w), 918 (w), 857 (m), 779 (s), 709 (m). Anal. Calcd for  $\text{C}_{12}\text{H}_7\text{AlClN}_2\text{O}_5\text{Pt}_{0.5} \cdot 1.1\text{CH}_3\text{CN}$ : C, 36.73; H, 2.24; N, 9.35. Found: C, 37.26; H, 2.75; N, 8.71. ICP determined for  $\text{C}_{12}\text{H}_7\text{AlClN}_2\text{O}_5\text{Pt}_{0.5} \cdot 1.1\text{CH}_3\text{CN}$  (referred as MOF-253-0.5Pt): Calcd: Al, 5.81; Pt, 21.01. Found: Al, 5.67; Pt, 21.31. Compound  $\text{C}_{12}\text{H}_7\text{AlCl}_{1.56}\text{N}_2\text{O}_5\text{Pt}_{0.78} \cdot 1.1\text{CH}_3\text{CN}$  (referred as MOF-253-0.78Pt) was obtained by using the same synthetic procedure as described for MOF-253-0.5Pt except that *cis*-Pt(DMSO) $_2\text{Cl}_2$  (0.4771 g, 1.136 mmol). The Pt/Al ratio was determined by ICP-MS to be 0.78.

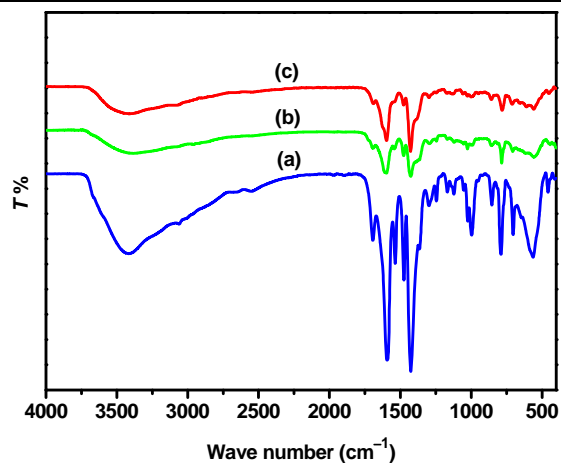


**Fig. S1** IR spectra of (a) MOF-253, (b) MOF-253-Pt before photocatalytic reaction and (c) MOF-253-Pt after photocatalytic reaction.

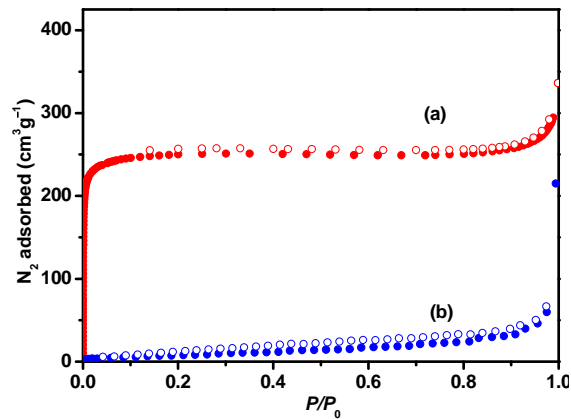


**Fig. S2**  $\text{N}_2$  adsorption ( $\bullet$ ) and desorption ( $\circ$ ) isotherms for (a) MOF-253 and (b) MOF-253-Pt.

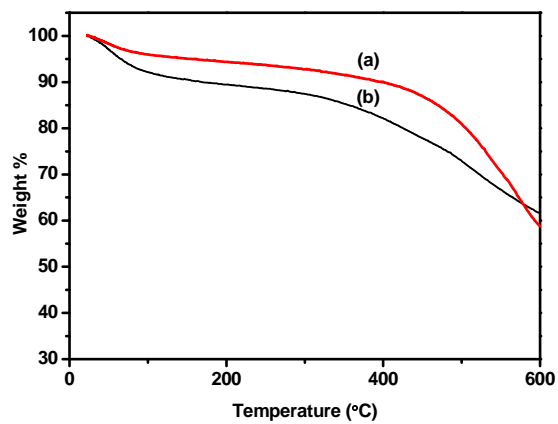


**Fig. S3** Thermogravimetric analysis results of (a) MOF-253 and (b) MOF-253-Pt.

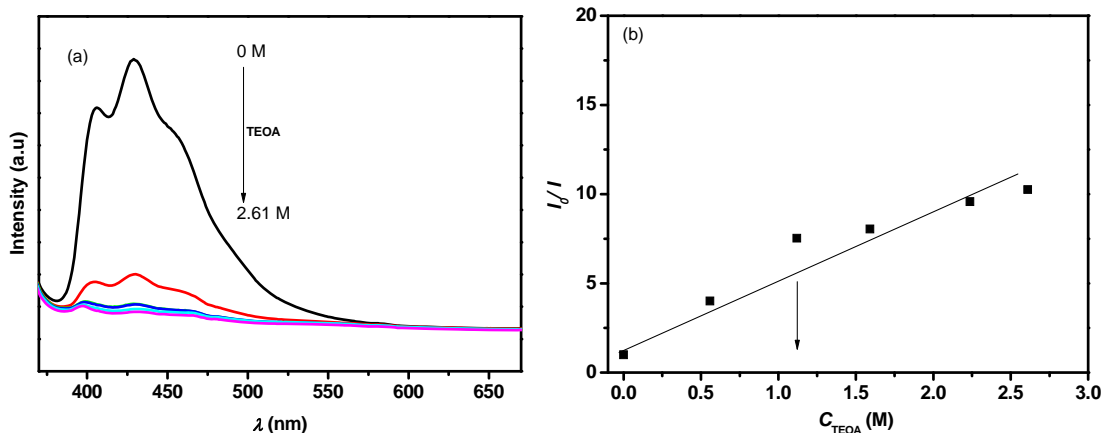


**Fig. S4** (a) Emission quenching of MOF-253-Pt (0.32 mM based on Pt) dispersed in Ar degassed CH<sub>3</sub>CN at room temperature with the concentration of TEOA varied from 0, 0.56, 1.12, 1.59, 2.24 to 2.61 M, respectively ( $\lambda_{\text{ex}} = 355$  nm). (b) Stern–Volmer plots for MOF-253-Pt (0.32 mM based on Pt) dispersed in Ar degassed CH<sub>3</sub>CN upon addition of TEOA at  $\lambda_{\text{em}} = 430$  nm ( $\lambda_{\text{ex}} = 355$  nm). The arrows indicate the concentration of TEOA used for H<sub>2</sub> production experiments. The data of emission quenching were analyzed based on the results shown in Fig. S4a.

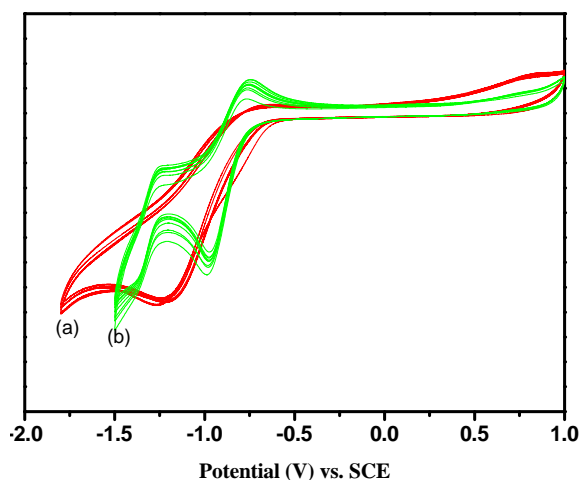


**Fig. S5** Cyclic voltammograms of (a) MOF-253 (red) and (b) MOF-253-Pt (green) in N<sub>2</sub>-purged CH<sub>3</sub>CN with 0.1 M Bu<sub>4</sub>NPF<sub>6</sub> at a scan rate of 100 mV/s. Note: The first reduction is the reduction of the pyridine (referred to as bpy) ligand attached to the Pt(II) ion  $E(\text{bpy}/\text{bpy}^-)$ . The second reduction peak is assigned to the Pt<sup>II</sup>/Pt<sup>I</sup> couple. The energy values of HOMO ( $E_{\text{HOMO}} = -6.201$  eV) and LUMO ( $E_{\text{LUMO}} = -3.881$  eV) of MOF-253-Pt have been calculated according to the equation below based on Solid state optical absorption spectrum of MOF-253-Pt and the first redox potential in Fig. S5.

$$E_{\text{LUMO}} = -|eE_{1/2} + 4.5eV + E_{\text{SCE}}| = -|eE_{1/2} + 4.741eV|$$

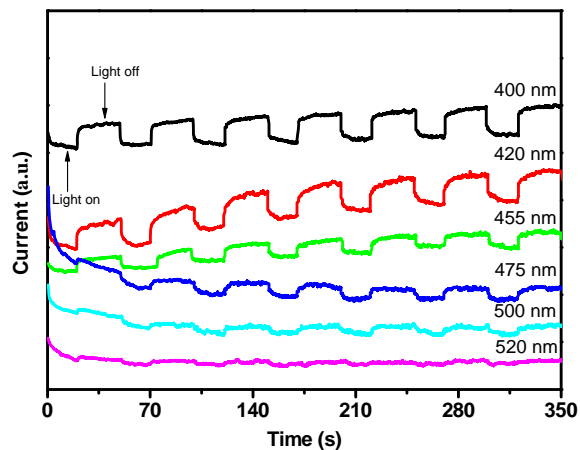


**Fig. S6** The photocurrent for the MOF-253-Pt electrode with different wavelength of the incident light. The wavelength of the incident light was controlled by using different cutoff filters ( $\lambda > 400, 420, 455, 475, 500,$  and  $520$  nm). The light source was a 300 W Xenon lamp. The photocurrent was recorded in 0.25 M  $\text{Na}_2\text{SO}_4$  aqueous solution containing 0.01 M TEOA under a constant potential of 0.35 V versus SCE.

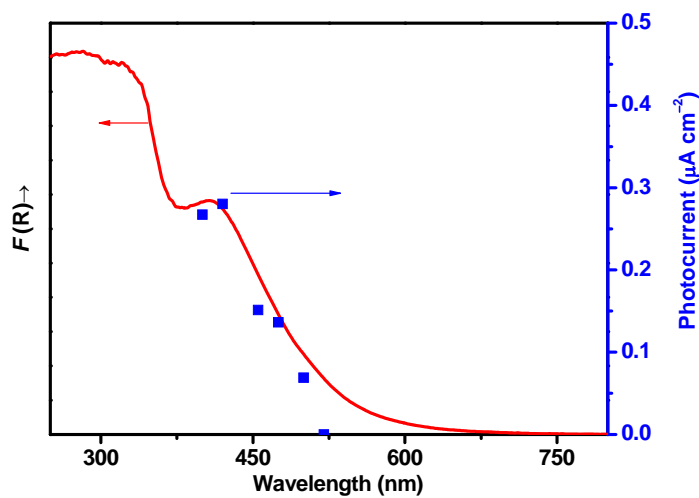


**Fig. S7** The dependence of photocurrent for the MOF-253-Pt electrode on the wavelength of incident light and UV-vis spectrum of MOF-253-Pt.

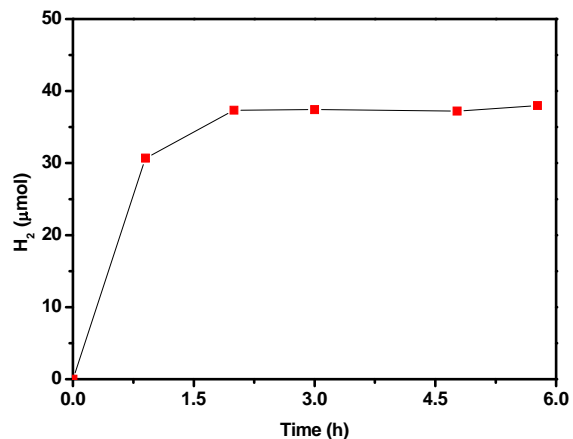


**Fig. S8** Photocatalytic H<sub>2</sub> evolution over MOF-253-Pt (0.53 mM based on Pt) in a 0.1 M acetate buffer solution (pH = 5) containing 30 mM EDTA. Other reaction conditions: 100 mL solution, light source: 300 W Xe lamp with 420 nm cut-off filter.

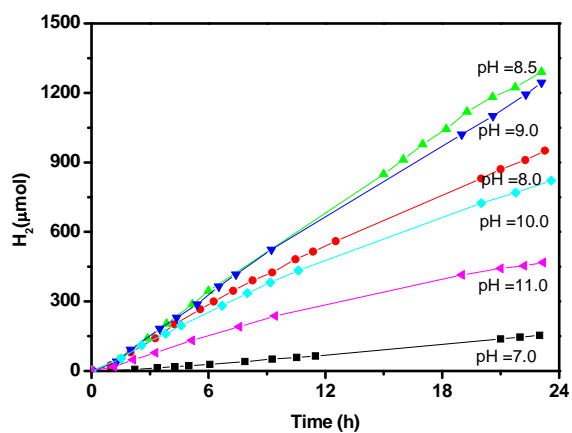


**Fig. S9** Photocatalytic H<sub>2</sub> evolution over MOF-253-Pt (0.53 mM based on Pt) in aqueous solution at different pH values. Other reaction conditions: 15% TEOA (v/v), 100 mL solution, light source: 300 W Xe lamp with 420 nm cut-off filter.

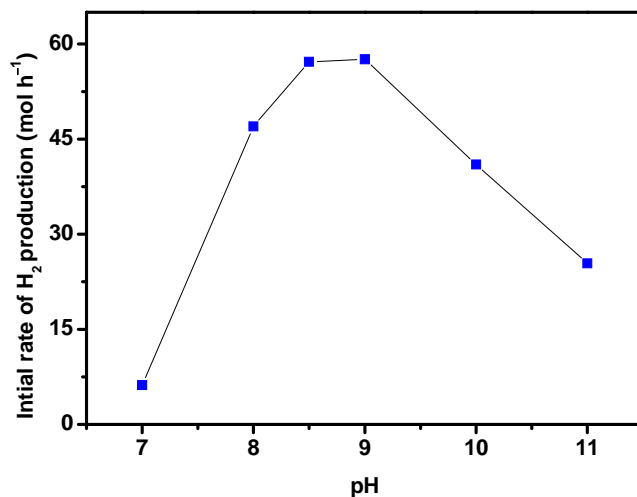


**Fig. S10.** Effect of pH on the initial rate of photocatalytic H<sub>2</sub> evolution over MOF-253-Pt. The data were analyzed based on the results of Fig. S9.

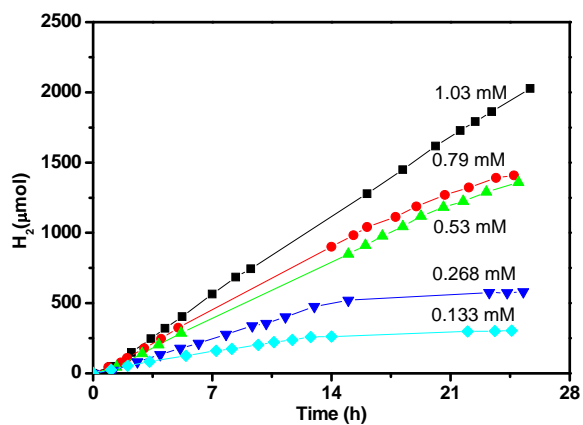


**Fig. S11** The effect of the concentration of MOF-253-Pt on H<sub>2</sub> evolution. Other reaction conditions: 15% TEOA (v/v), pH 8.5, 100 mL solution, light source: 300 W Xe lamp with 420 nm cut-off filter.

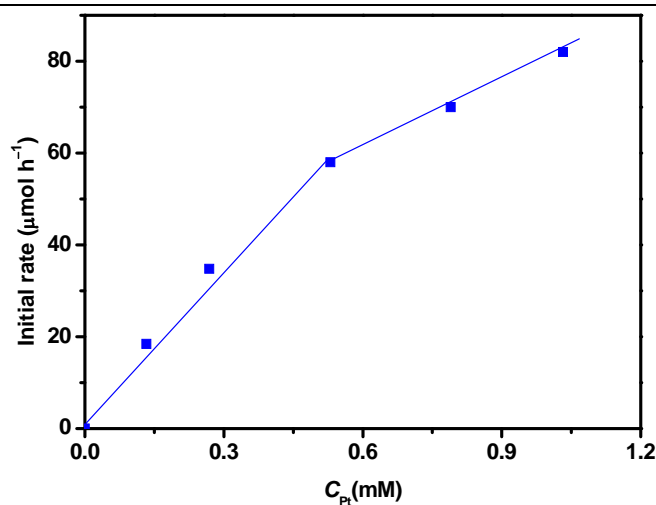


**Fig. S12** Variation of the initial rate of  $\text{H}_2$  evolution with the concentration of MOF-253-Pt. Other reaction conditions: 15% TEOA (v/v), pH 8.5, 100 mL solution, light source: 300 W Xe lamp with 420 nm cut-off filter. The data were analyzed based on the results in Fig. S11.

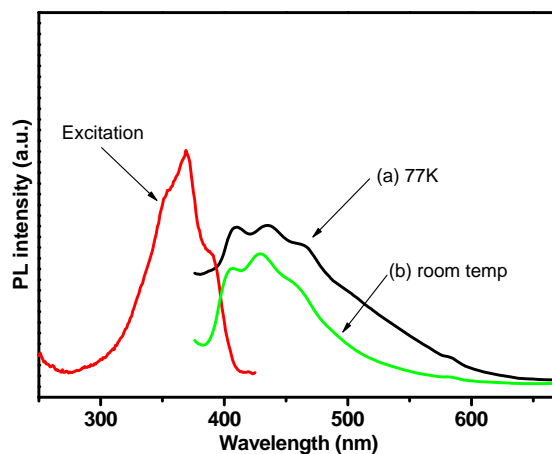


**Fig. S13** Photoluminescence spectra of MOF-253 in  $\text{CH}_3\text{CN}$  at (a) 77 K and at room temperature (b),  $\lambda_{\text{ex}} = 355$  nm.

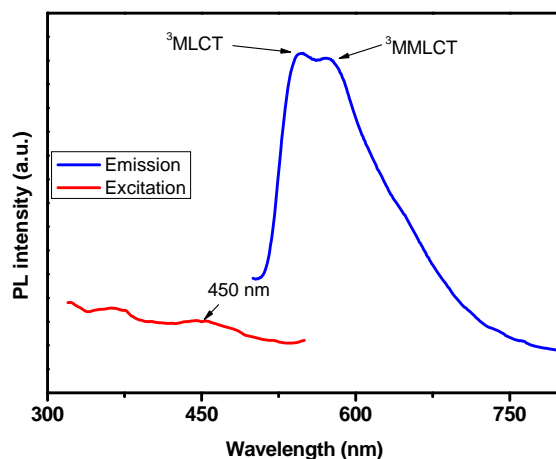


**Fig. S14** Photoluminescence spectra of MOF-253-Pt dispersed in Ar degassed CH<sub>3</sub>CN at 77 K, λ<sub>ex</sub> = 450 nm.

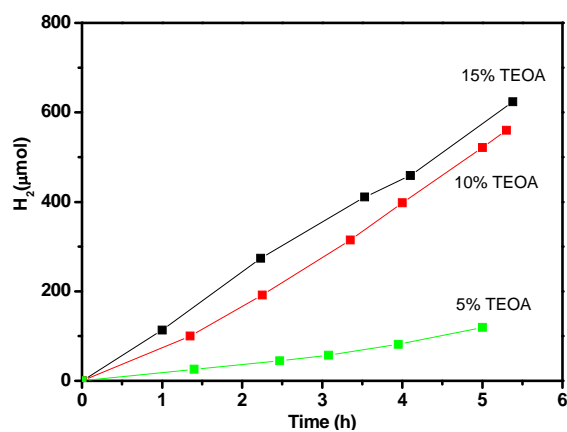


**Fig. S15** The effect of TEOA concentration on photocatalytic H<sub>2</sub> evolution over MOF-253-Pt (1.03 mM) in CH<sub>3</sub>CN/H<sub>2</sub>O (1:1, v/v). Other reaction conditions: pH 8.5, 100 mL solution, light source: 300 W Xe lamp with 420 nm cut-off filter.

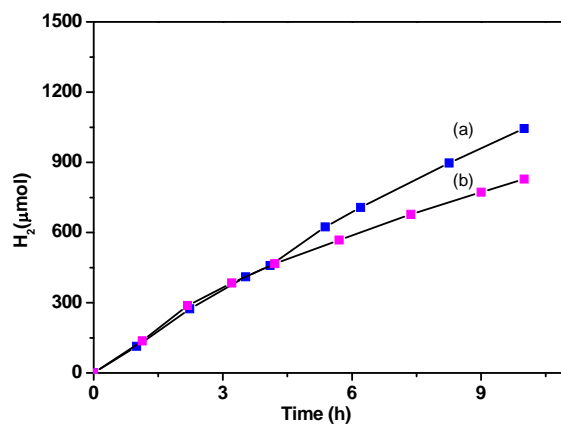


**Fig. S16** Photocatalytic H<sub>2</sub> evolution over MOF-253-Pt (1.03 mM) in CH<sub>3</sub>CN/H<sub>2</sub>O (1:1) in (a) the absence and (b) the presence of mercury (0.5 mL). Other reaction conditions: 15% TEOA (v/v), pH 8.5, 100 mL solution, light source: 300 W Xe lamp with 420 nm cut-off filter.

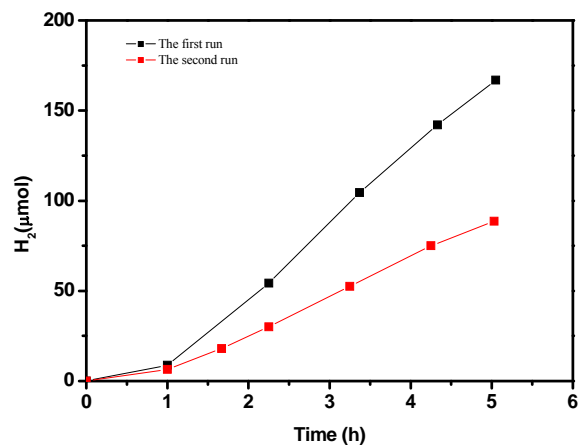


**Fig. S17** Photocatalytic hydrogen production from systems containing MOF-253-Pt (0.53mM) in mixed solvent of CH<sub>3</sub>CN/TEOA/H<sub>2</sub>O (17:2:1) (100 mL) at pH 8.5 upon irradiation with 300 W Xe lamp ( $\lambda > 420$  nm, 100 mL solution).

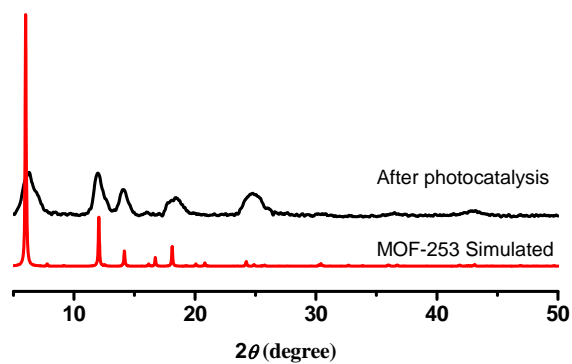


**Fig. S18** Powder X-ray diffraction patterns for simulated MOF-253 and MOF-253-Pt after photocatalytic reaction.

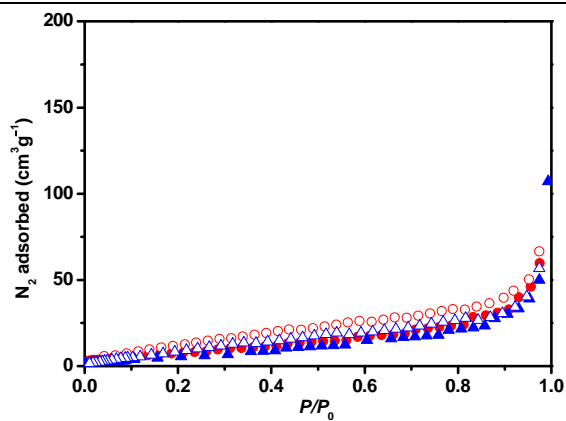


**Fig. S19** N<sub>2</sub> adsorption (●, ▲) and desorption (○, △) isotherms for MOF-253-Pt before photocatalytic reaction (●, ○) and MOF-253-Pt after photocatalytic reaction (▲, △). The Langmuir surface area and pore volumes at a relative pressure of 0.994 bar to be 255 m<sup>2</sup> g<sup>-1</sup> and 0.166 cm<sup>3</sup> g<sup>-1</sup> for MOF-253-Pt after photocatalytic reaction, respectively.

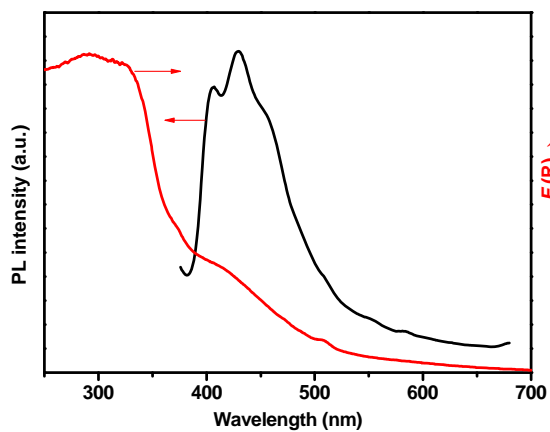


**Fig. 20** Photoluminescence ( $\lambda = 355$  nm) and UV-vis spectra of MOF-253-Pt after photocatalytic reaction. The UV-vis spectrum show that Pt may be partially leached into solution via the detachment of PtCl<sub>2</sub> moieties from the bipyridine group in the MOF framework.

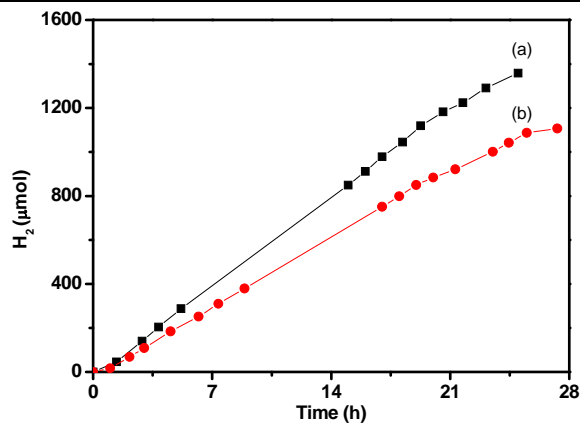


**Fig. 21** The effect of Pt loading in MOF-253 on photocatalytic H<sub>2</sub> evolution including (a) 0.53 mM based on Pt (MOF-253-0.5Pt) and (b) 0.73 mM based on Pt (MOF-253-0.78Pt) in TEOA aqueous solution. Other reaction conditions: pH 8.5, 100 mL solution, light source: 300 W Xe lamp with 420 nm cut-off filter. **Note:** The rate and amount of hydrogen production at higher Pt loading (Curve b) is lower than those at lower Pt loading (Curve a), suggesting that Pt complex within the pores of MOF-253-0.78Pt could be less accessible to the water molecules due to more extensive pore blockage.

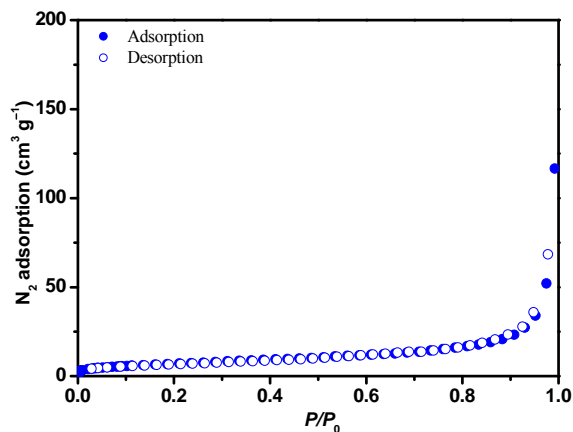


**Fig. S22** N<sub>2</sub> adsorption (●) and desorption (○) isotherms for MOF-253-0.78Pt. The Langmuir surface area and pore volumes at a relative pressure of 0.994 bar to be 95.7 m<sup>2</sup> g<sup>-1</sup> and 0.181 cm<sup>3</sup> g<sup>-1</sup>, respectively.

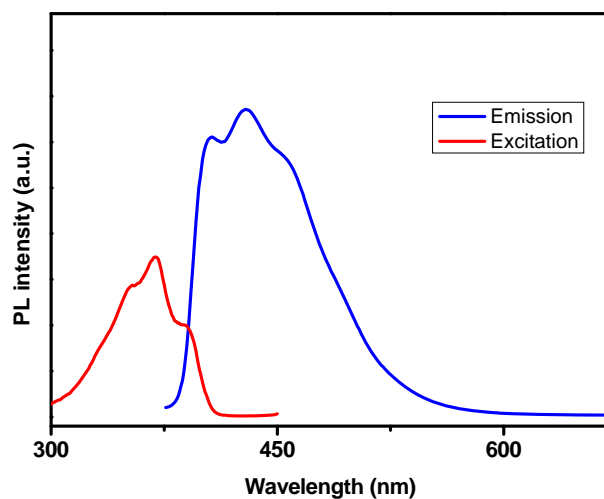


**Fig. S23** Photoluminescence spectra of Pt(bpydc)Cl<sub>2</sub> dispersed in Ar degassed CH<sub>3</sub>CN at room temperature,  $\lambda_{\text{ex}} = 355$  nm.

**References:**

1. J. H. Price, A. N. Williamson, R. F. Schramm, B. B. Wayland, *Inorg. Chem.* 1972, **11**, 1280-1284.
2. A. Islam, H. Sugihara, K. Hara, L. P. Singh, R. Katoh, M. Yanagida, Y. Takahashi, S. Murata, H. Arakawa and G. Fujihashi, *Inorg. Chem.* 2001, **40**, 5371-5380.
3. X.-B. Zhang, J.-M. Yan, S. Han, H. Shioyama and Q. Xu, *J. Am. Chem. Soc.* 2009, **131**, 2778-2779.